The Vibrating Ellipse-Shaped Drum

Michael Trott, Wolfram Research, Inc.

The Laplace equation for an ellipse is solved by the method of separation of variables. The resulting one-dimensional differential equations are solved with Mathieu functions. The eigenvalues are calculated numerically and the various kinds of eigenmodes are visualized with 3D and contour plots. Some degenerate eigenmodes are explicitly calculated.

The vibrating rectangle and the vibrating circular drum are the two best known examples where the Helmholtz equation can be solved by the method of separation of variables. Here, we will consider the case of a vibrating ellipse-shaped drum. This problem is slightly more complicated because, after separation of variables, the resulting ordinary differential equations are Mathieu equations.

Let us consider a membrane inside an ellipse-shaped region with the membrane held fixed at the boundary. The displacement $u(\mathbf{r}, t)$ of the membrane is governed by the wave equation

$$\Box u(\mathbf{r}, t) = \Delta u(\mathbf{r}, t) - \frac{1}{c^2}\frac{\partial^2 u(\mathbf{r}, t)}{\partial t^2} = 0$$

Assuming harmonic time dependence $u(\mathbf{r}, t) = \psi(\mathbf{r}) \cos(\omega t)$, the wave equation can be separated. In this article, we will solve the $\mathbf{r}$-dependent eigenvalue problem.

Let $\lambda = \omega / c$ and let a and b be the half-axes of the ellipse. Let Ω denote the interior region,

$$\Omega = \left\{ \mathbf{r} = (x, y) : \frac{x^2}{a^2} + \frac{y^2}{b^2} < 1 \right\}$$

and let $\partial\Omega$ denote the boundary. Then the equations under consideration are

$$-\Delta\psi_n(\mathbf{r}) = \lambda_n^2\, \psi_n(\mathbf{r}) \quad \text{for} \quad \mathbf{r} \in \Omega, \quad \psi_n(\mathbf{r}) = 0 \quad \text{for} \quad \mathbf{r} \in \partial\Omega$$

Separation of Variables

The Laplace operator separates in an elliptical coordinate system. An elliptical coordinate system (r, φ) is related to a Cartesian coordinate system by the equations

$$x = c \cosh r\, \cos\varphi, \quad y = c \sinh r\, \sin\varphi, \quad 0 \le \varphi \le 2\pi, \quad 0 < r < \infty$$

For a given ellipse, the half axes a and b are related to c and the maximal value r_0 of r by

$$a = c \cosh r_0, \quad b = c \sinh r_0$$

The curves $r = \textit{constant}$ are ellipses with foci at $\pm c$ and the curves $\varphi = \textit{constant}$ are hyperbolas. Here is a net of coordinate lines for $c = 1$.

```
In[1]:= With[{c = 1},
          Show[Graphics[{
            {RGBColor[1, 0, 0], Table[Line[
                Table[{c Cosh[r] Cos[φ], c Sinh[r] Sin[φ]},
              {φ, 0, 2 π, π/100.}]], {r, 0, 1, 1/15}]},
            {RGBColor[0, 0, 1], Table[Line[
                Table[{c Cosh[r] Cos[φ], c Sinh[r] Sin[φ]},
              {r, 0, 1, 0.01}]], {φ, 0, 2 π, π/19.}]}}],
          AspectRatio → Automatic,
          PlotRange → All, Frame → True]];
```

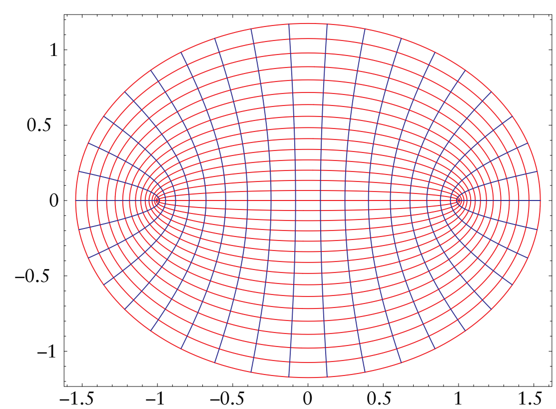

Calculation of Eigenvalues and Eigenfunctions

The "azimuthal" (φ dependent) equation derived above has arbitrary linear combinations of Mathieu functions as solutions. For physical reasons, we want the solutions to be periodic in φ. This implies a relation between a and q. The *Mathematica* commands `MathieuCharacteristicA`$[p, q]$ and `MathieuCharacteristicB`$[p, q]$ give values of a such that the corresponding Mathieu functions `MathieuC` and `MathieuS` are quasiperiodic with period π/p (this means they have the form $e^{ipz} g(z)$ with $g(z)$ a 2π-periodic function). We define the quasiperiodic Mathieu functions $ce_n(q, z)$ (for $n \ge 0$) and $se_n(q, z)$ (for $n > 0$) by

Michael Trott studied physics at the Humboldt University of Berlin from 1981 to 1986. He received his Ph.D. in theoretical solid state physics in 1990 at the Technical University of Ilmenau. In 1994, he joined the Research and Development team at Wolfram Research, Inc. His current scientific interests include visualization in mathematics, elliptic functions, the application of computer algebra to solved and unsolved problems in physics, and the foundational problems of quantum mechanics.

```
In[11]:= ce_n_Integer?NonNegative[q_, z_] =
           MathieuC[MathieuCharacteristicA[n, q], q, z];
         se_n_Integer?Positive[q_, z_] =
           MathieuS[MathieuCharacteristicB[n, q], q, z];
```

The solutions of the "radial" (r dependent) equation are also Mathieu functions, but with purely imaginary argument.

For $r = 0$, we must have continuity along the line connecting the two foci. Using the fact that ce_n is an even function that is nonzero at $z = 0$ and se_n is an odd function, we obtain the following forms for the eigenfunctions $\psi_n(r, \varphi)$:

$$\psi^c_{n\,j}(r, \varphi) \propto ce(q^c_{n\,j}, \varphi)\, ce(q^c_{n\,j}, ir),\ n = 0, 1, 2, \ldots, j = 1, 2, \ldots$$
$$\psi^s_{n\,j}(r, \varphi) \propto se(q^s_{n\,j}, \varphi)\, se(q^s_{n\,j}, ir),\ n, j = 1, 2, \ldots$$

The corresponding eigenvalues are given by

$$\lambda^c_{n\,j} = 2\sqrt{q^c_{nj}/c}, \qquad \lambda^s_{n\,j} = 2\sqrt{q^s_{nj}/c}$$

The Dirichlet boundary condition at $r = r_0$ remains to be fulfilled. For definiteness, we will take $r_0 = 2/3$.

```
In[13]:= r0 = 2/3;
```

The boundary conditions gives a countable number of $q_{n\,j}$ for a given r_0 and fixed n. We will find such values numerically.

Looking at a typical example, we see that certain values of q satisfy the boundary condition for $n = 2$:

```
In[14]:= Plot[ce2[q, I r0], {q, 0, 25}];
```

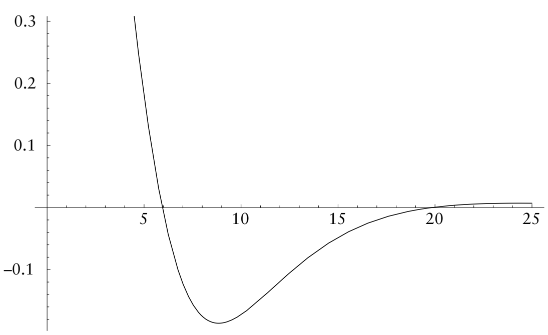

We can use this plot to approximate the zeros by selecting the intervals where the function value changes sign.

Lyapunov Exponents

Lyapunov exponents provide a quantitative measure of the divergence or convergence of nearby trajectories for a dynamical system. If we consider a small hypersphere of initial conditions in the phase space, for sufficiently short time scales, the effect of the dynamics will be to distort this set into a hyperellipsoid, stretched along some directions and contracted along others. The asymptotic rate of expansion of the largest axis is measured by the largest LCE λ_1. In general, if we sort the axes and LCEs in decreasing order by magnitude ($\varepsilon_1 \geq \cdots \geq \varepsilon_n$ and $\lambda_1 \geq \cdots \geq \lambda_n$), each λ_i quantifies the average exponential rate of expansion or contraction for the i-th axis ε_i.

algebraic number	polynomial divisible by its minimal polynomial
$a + b$	$\text{Resultant}_y\,(f(x - y),\, g(y))$
$a - b$	$\text{Resultant}_y\,(f(x + y),\, g(y))$
$a \cdot b$	$\text{Resultant}_y\,(y^{\deg(f)}\, f(x/y),\, g(y))$
a/b	$\text{Resultant}_y\,(f(x\,y),\, g(y))$
$a^{p/q}$	$\text{Resultant}_y\,(f(y),\, x^q - y^p)$

TABLE 1.

An n-dimensional *continuous-time* (autonomous) smooth dynamical system is defined by the differential equation

$$\dot{x} = F(x), \tag{1}$$

More formally, consider two nearby points x_0, $x_0 + u_0$ in the phase space M, where u_0 is a small perturbation of the initial point x_0 (see Figure 1). After a time t, their images under the flow will be $f^t(x_0)$ and $f^t(x_0 + u_0)$ and the perturbation u_t will become

$$u_t \equiv f^t(x_0 + u_0) - f^t(x_0) = D_{x_0}\, f^t(x_0) \cdot u_0, \tag{2}$$

where the last term is obtained by linearizing f^t. Therefore the average exponential rate of divergence or convergence of the two trajectories where $\|u\|$ denotes the length of a vector u. If $\lambda(x, u) > 0$, then one has exponential divergence of nearby orbits. It can be shown that, under very weak smoothness conditions on the dynamical system, the limit exists and is finite for almost all points $x_0 \in M$, and, for almost all tangent vectors u_0, it is equal to the largest LCE λ_1 [Oseledec 1968].

Following the algorithm of [Benettin et al. 1980], we start by choosing an initial condition x_0 and an $n \times n$ matrix $U_0 = [u^0_1, \ldots, u^0_n]$. Using the Gram-Schmidt procedure, we calculate the corresponding matrix of orthonormal vectors $V_0 = [v^0_1, \ldots, v^0_n]$ and integrate the variational equation (7) from $\{x_0, V_0\}$ for a short interval T, to obtain $x_1 = f^T(x_0)$ and

$$U_1 \equiv [u^1_1, \ldots, u^1_n] = D_{x_0}\, f^T(U_0) = \Phi_T(x_0) \cdot [u^0_1, \ldots, u^0_n].$$

Again, we calculate the orthonormalized version of U_1 and integrate the equation from $\{x_1, V_1\}$ for T seconds to obtain x_2 and U_2. We repeat this integration-orthonormalization procedure K times.

$$\sum_{p(r)=0} f(r)/g(r) = -a_1/a_0.$$

Let us describe two necessary subalgorithms. First, we need an algorithm to perform arithmetic operations on isolating rectangles. It is well known how to perform arithmetic on real intervals. Now suppose that we have two rectangles in the complex plane, $R = A + B \cdot i$ and $S = C + D \cdot i$, where A, B, C, and D are real intervals. To add, subtract, multiply, or divide R and S, or raise R to a natural power n, we use the following facts (for the division R/S, we assume that the closure of S does not contain zero):

$$R \pm S = (A \pm C) + (B \pm D)\, i$$
$$R \cdot S \subseteq (AC - BD) + (AD + BC)\, i$$

$$R/S \subseteq (AC+BD)/(C^2+D^2) + (BC-AD)/(C^2+D^2)\; i$$

$$R^n \subseteq \sum_{k=0}^{[n/2]} \binom{n}{2k} (-1)^k\, A^{n-2k} B^{2k}$$
$$+\, i \sum_{k=0}^{[(n-1)/2]} \binom{n}{2k+1} (-1)^k\, A^{n-2k-1} B^{2k+1}$$

In addition, we need an algorithm for making an isolating rectangle of an algebraic number a smaller. A rectangle bisection method was suggested in [Collins and Krandick 1992]. We also use the following hybrid method:

1. Try to compute a numeric approximation of a by supplying the middle point of the isolating rectangle R as a starting point of the second stage of the Jenkins-Traub algorithm.
2. If the numeric algorithm does not converge, go to step 4.
3. Use Lemma 1 to find a rectangle R_1 containing at least one root of the minimal polynomial of a. If $R_1 \subset R$, put $R := R_1$ and go to step 5; else, go to step 4.
4. Bisect R several times.
5. If the new R is sufficiently small, return R; else, go to step 1 with increased precision of computations.

The computing time of the rectangle bisection method grows much faster with the required precision than the computing time of the hybrid method. However, the rectangle bisection method is more effective when we need to make large rectangles only a few bisections smaller.

Visualization of the Eigenfunctions

Having calculated some explicit numerical values for the eigenvalues (that is, for q), let us take a look at the form of the corresponding displacements. We define a function `EigenfunctionsPlot3D` which makes a 3D picture of the eigenfunctions. The graphics object `boundary` represents the fixed boundary of the membrane.

```
In[22]:= boundary =
           {Thickness[0.01],
            Line[Table[{Cosh[r0] Cos[φ], Sinh[r0] Sin[φ], 0},
              {φ, 0, 2π, 2π/200.}]]};
```

Here are some examples.

```
In[26]:= EigenfunctionsPlot3D[ψc[0, 1, r, φ], {r, φ}]
```

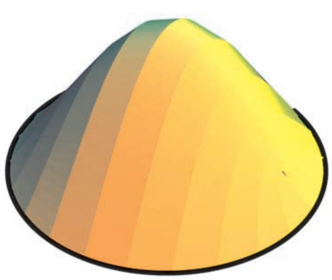

```
In[28]:= EigenfunctionsPlot3D[ψc[1, 1, r, φ], {r, φ}]
```

Using more `PlotPoints`, we can also visualize higher-lying states. The following picture shows the state $\psi^{c}_{24\,1}$ calculated above. It has the remarkable property that the displacement is mainly concentrated at the boundary and the middle is quite flat. This is a "whispering gallery" state, so called by Lord Rayleigh, who observed that in certain rooms sound waves can travel along the walls.

```
In[31]:= EigenfunctionsPlot3D[ψs[24, 1, r, φ], {r, φ},
           PlotPoints → 125]
```

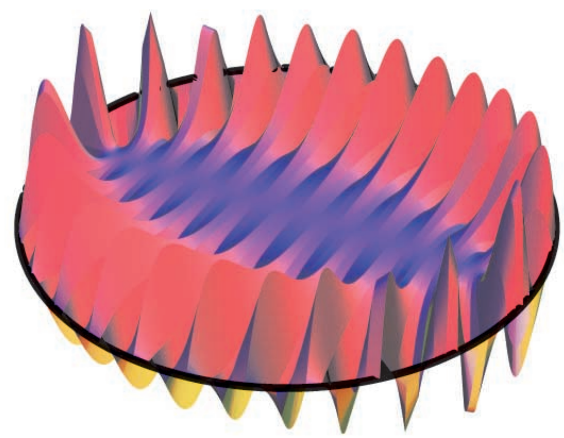

Figure 1 shows an animation of the time-dependent vibrations for the mode $\psi^{c}_{3\,2}$.

Here are three examples of contour plots of the eigenfunctions calculated above.

```
In[36]:= EllipseContourPlot[ψc[2, 2, r, φ], {r, φ},
           ColorFunction → Hue, PlotPoints → 50];
```

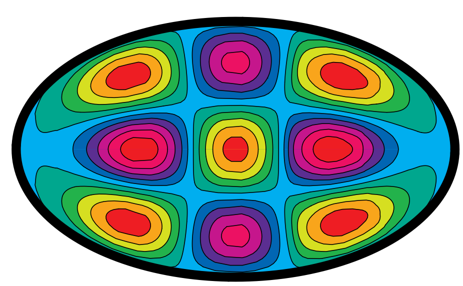

```
n[38]:= EllipseContourPlot[ψs[5, 2, r, φ], {r, φ},
          ColorFunction → (Hue[Random[]]&), PlotPoints → 50];
```

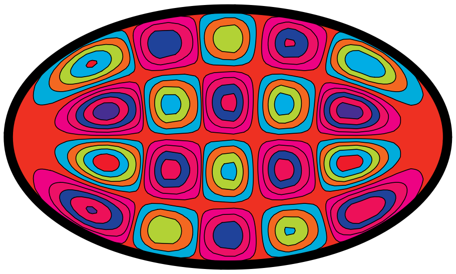

Degeneracies

In comparison to a circular membrane, the ellipse-shaped membrane has an extra degree of freedom, the eccentricity of the ellipse. By varying the eccentricity, one can obtain the situation where two states have the same eigenvalue, which means the same q.

Here are the first few states calculated for 10 different values of r_0. The starting values for the numerical root findings are recursively reused.

This plot shows the dependence of the states on r_0.

```
n[40]:= Show[Graphics[{
            Table[MapIndexed[{
              Hue[(#2[[1]] - 1)/3], Line[#1]}&,
              ρListc[i]], {i, 0, 5}],
            Circle[{0.723, 31.9}, {0.005, 0.85}]}],
          PlotRange → All, Frame → True,
          FrameLabel → {"r", "q"}];
```

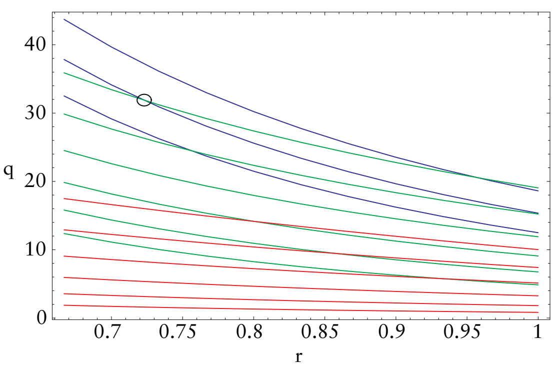

The circle indicates one point of degeneracy of λ^{c}_{13} and λ^{c}_{52}. Let us calculate this point more accurately.

```
In[41]:= r* = r /. FindRoot[
            (q /. FindRoot[ce1[q, I r] == 0, {q, 31, 33}]) ==
             (q /. FindRoot[ce5[q, I r] == 0, {q, 31, 33}]),
            {r, 0.7, 0.8}]
Out[41]= 0.72257
```

The corresponding value of q is:

```
In[42]:= q* = q /. FindRoot[Evaluate[ce1[q, I r*] == 0], {q, 31, 33}]
Out[42]= 31.9028
```

Because the eigenvalues λ^{c}_{13} and λ^{c}_{52} are the same for $r = r_*$, the general form of the eigenfunctions is a linear combination of these two states, $\lambda^{c}_{13} + \mu\, \lambda^{c}_{52}$. The large factor 300 in the following formula accounts for the fact that the two eigenfunctions are not normalized.

```
In[43]:= ψ*[μ_, r_, φ_] :=
            300 μ ce1[q*, φ] ce1[q*, I r] +
              (1 - μ) ce5[q*, φ] ce5[q*, I r];
```

By varying the value of μ, we get various resulting shapes for the displacements.

References

Arscott, F.M. 1964. *Periodic Differential Equations*. New York: MacMillan.

Chen, G., P.M. Morris, and J. Zhou. 1994. *SIAM Review* 56:453.

McLachlan, N.M. 1947. *Theory and Applications of Mathieu Functions*. Clarendon Press, Oxford.

Michael Trott
Wolfram Research, Inc.
100 Trade Center Drive, Champaign, IL 61820

The electronic supplement contains the Version 3.0 notebook `EllipseShapedDrum.nb`.